Unconventional Approach to Estimate Permeability of Thin Beds in a Carbonate Reservoir with Vertical Interference Testing*

Christophe Bassem Maalouf[1], Salem Al Jaberi[1], Irina Baca Espinoza[1], F.Elarouci[2], S. Smith[2], and H.Khairy[2]

Search and Discovery Article #41834 (2016)**
Posted August 22, 2016

*Adapted from extended abstract prepared in relation to oral presentation at GEO 2016, 12th Middle East Geosciences Conference and Exhibition, Manama, Bahrain, March 7-10, 2016. Bahrain:
Please refer to related article by the first author and colleagues, Search and Discovery Article #41833 (2016).

[1]ADMA-OPCOd, Abu Dhabi, UAE (bassem.maalouf@gmail.com)
[2]Baker Hughes, Abu Dhabi, UAE

Abstract

The evaluation of permeability across heterogeneous layer-cake reservoirs is challenging. For such cases, pressure-transient-analysis interpretation from well testing is usually not very reliable, because it can derive only average permeability. The vertical interference tests (VITs) conducted by wireline formation testing (WFT) can be one of the best solutions to evaluate the reservoir communication, anisotropy ratio, and zonal horizontal permeability. However, the standard method of homogeneous single-layer interpretations might not work well for zones with thin beds in between.

This article describes an unconventional approach for how VIT data was managed to interpret a multilayer zone in a carbonate green field offshore Abu Dhabi. Three tests were performed to measure the permeability within the layered reservoir and across a thin stylolite in between two layers. The initial pressure-derivative modelling with standard assumptions did not give a good match; so additional methods were evaluated. The new approach is based on integrated analysis, including core data analysis using a modified Lorenz Plot, associated hydraulic flow units, and reservoir quality index, an analytic permeability log from nuclear magnetic resonance (NMR) and WFT pretest mobility. The result of the tight-zone analysis was improved using the VIT data across all layers with higher complexity and enables matching pressure derivatives with a more realistic interpretation.

The revised pressure-transient analysis gave a better match that was not possible using the homogeneous model. Additional data from vertical flow units and analytic permeability logs were used to fine-tune the multilayer models. The permeability findings matched the core data from offset wells. The results showed improved accuracy for horizontal and vertical permeability, thus providing improved understanding of zonal productivity which was crucial for the field development strategy. The successful approach of using wireline open-hole logs and conventional core analysis from offset wells enables the generation of finely tuned multilayer models for VIT interpretation.

Introduction

Quantitative permeability measurements are as central to field development as inputs are for static models. These measurements vary in methodology and applicability and are well documented; however, the heterogeneous carbonates of the Middle East pose unique challenges to obtaining accurate and useful permeability measurements. Standard well tests performed over large intervals provide average permeability values, but the true distribution is much more varied. As the grid size for static models increases in density to accurately optimize individual layer development, the more necessary it is to have accurate mapping of the permeability at a higher resolution. One method for improving the resolution is the Vertical Interference Test (VIT) performed with a Wireline Formation Tester (WFT) and using Pressure Transient Analysis (PTA) to obtain an analytical solutions for horizontal (Kxy) and vertical (Kz) permeability. A full description of this method is beyond the scope of this article, but the procedure and theoretical basis is documented in the literature (Al-Amrie, Ben-Saad, et al., 2012). A VIT can be used to calculate a quantitative value for horizontal and vertical permeability over an interval as little as approximately 6.5 ft.

However, thin stylolites below the resolution of the VIT can act as baffles or barriers in layered carbonates, and determining the impact and behavior of these in between the higher permeability producing zones requires additional input and analysis. One common application in this environment is conducting the VIT across the stylolite to measure the communication across the low-permeability zone. In the case of a barrier where no communication is detected, this method is sufficient. However, where there is communication across the stylolite, the resulting analysis becomes more complex because a layered model is needed to represent the formation and the Kxy and Kz for each layer is unknown. Finding an analytical solution for horizontal and vertical permeability values in each layer is very difficult.

This situation with a thin stylolite separating permeable zones was addressed in a local reservoir. The approach integrated core data analysis using a Modified Lorenz Plot, associated hydraulic flow units and reservoir quality index, analytic permeability data from nuclear magnetic resonance (NMR) and WFT pretest mobility. The result of the analysis across the stylolite was improved using the integrated data with the VIT data in a more complex multi-layered model.

Background

The field was discovered with Well-1 in 1971 and was subsequently appraised with 11 wells drilled between 1975 and 2014. The reservoir is a layer-cake oil/wet carbonate with six productive layers interbedded with five baffles in the oil zone and one microporous low-permeability layer at the bottom of the oil zone (Figure 1). Productive layers are approximately10-ft thick, whereas baffles are approximately2-ft thick. The bottom layer is approximately 24-ft thick. These layers are homogeneous laterally across the field. A thin stylolite zone is interbedded between the bottom two layers, referred to as Layers A and C in this article (Figure 2). The objective of the VIT was to evaluate the dynamic communication between A and C and the dynamic role of the stylolite.

Data Review

A full suite of logging data was acquired throughout the interval of interest, including gamma-ray, array resistivity, density, neutron, NMR, full waveform acoustic and image log data (electrical and acoustic). Pore pressure and mobility measurements were conducted with a WFT, in addition to the VITs. Processed log data throughout the interval is shown in Figure 3 by highlighting layers A and C.

Three VITs were conducted throughout the interval containing the lowest water-bearing zone, the overlying low-permeability stylolite, and the hydrocarbon-bearing zone immediately above. Each VIT was conducted over a slightly different interval and provided various information about the layers. Quality control of all the VIT data indicated the data was of good quality and sufficient for analysis.

The objective of VIT-1 was to prove dynamic communication between layers A and C. It was a probe-to-probe test. The upper probe was set in Layer-A and the lower probe was set in Layer-C, across the low permeability Layer-B (Figure 4). The upper probe was used as the producing source and the lower probe was used for observation, and the distance between the probes was 14 ft. Using the upper probe, 55L were pumped from the formation over 5 hours. The pressure drawdown ranged from 1300 to 2350 psi at the producing probe, causing a pressure drop of only 0.8 to 1.3 psi at the observation probe. The fluid at the producing probe was estimated as 60% oil and 40% water-based mud filtrate. An oil sample was collected through the producing probe at the end of the pump-out, using selective sampling of the segregated oil slug. The test confirmed communication across the low-permeability stylolite Layer B; however, because of the large distance (14 ft) between the probes and the small drawdown observed at the observation probe, the pressure change was not sufficient for quantitative pressure transient analysis and no build-up was performed. The flowing pressure data was analyzed using a homogeneous model to obtain an average permeability range over the interval tested. Figure 5 and Table 1 summarize the results.

VIT-2 was performed within Layer-A, also using two probes (Figure 6) in order to measure the average permeability (Kxy and Kz), using PTA with a homogeneous model. In this test, the probes were separated by 9.5 ft, and the upper probe was used as the producing (source) probe while the lower probe was used for observation. The pump-out duration was approximately 1.5 hours and the build-up duration was approximately 1.75 hours. After an initial high drawdown during the early cleaning period, an average pressure drop of 250 psi at the producing probe resulted in a 3.3 psi pressure drop at the observation probe (Figure 7).

In this analysis, the upper and lower boundaries of Layer-A were specified as ‘no-flow’ boundaries which has some impact on the analysed result because the upper boundary of Layer-A is not well defined and the previous test confirmed communication across the lower boundary (Layer-B) (so some response is expected from these intervals). An indication of this is observed on the log-log plot at the end of the build-up period, where there is a slight downward trend of the derivative (Figure 8). Between approximately 100 to 400 seconds, the derivative indicates radial flow on both the producing and the observation probes, and therefore the measurement represents the average permeability across the interval tested between the two probes (Table 2).

In VIT-1, the pressure drop at the observation probe was only approximately 1 psi. In order to confirm VIT-1 results, it was decided to perform VIT-3 across Layer-B using a standard tool configuration, where a straddle packer module was used as the producing source, set in Layer-C, and the observation probe was set in the lower part of Layer-A (Figure 9). Therefore, VIT-3 was a repeat of VIT-1 but with a different tool

configuration. The distance between the straddle packer and the observation probe was approximately 10 ft. A pressure drop of 2.8 psi was measured at the observation probe in Layer-A as a result of approximately 250 psi drawdown pressure at the straddle packer in Layer-C (Figure 10).

A homogeneous model was used to analyze the build-up pressure data from the straddle packer and probe where a satisfactory match with the straddle-packer gauge was obtained. The match for the observation probe data is not as good (Figure 11). More importantly, the analysis results using this model can only provide an average permeability over the interval, which includes responses from Layers A, B and C.

Data Integration

Improved VIT analysis (e.g., Table 3) using PTA methodology required a more realistic multilayer model. Additional data was integrated to create the initial model and was also used to refine the subsequent VIT analysis. Core analysis from a nearby offset well provided an indication of horizontal and vertical permeability magnitudes, and processed NMR data from the current well was also reviewed to identify basic rock types. The rock types, defined as a stratigraphically continuous interval of similar reservoir process speed that maintains the geologic framework and characteristics (Gunter et al., 2004) were grouped into similar flow units (FU) which provided further insight into the reservoir dynamics.

Conventional core was acquired in the current well, but the analyzed results were not expected to be available until later; this would slow down field development planning. However, analyzed core data from an offset well was available covering Layer-A and Layer-C and with one core point representing Layer-B (Table 4). Using log data, the formations were not expected to have significant lateral variations in character; so the magnitude of this core data permeability was used as a reasonable calibration point for the NMR permeability index, and it also provided input to the sensitivity analysis for improved VIT processing. The permeability values indicate high heterogeneity in Layer-A and a more homogeneous formation in Layer-C.

Core Data

NMR Permeability Index

Nuclear Magnetic Resonance (NMR) data analysis gives a porosity distribution from various pore sizes and also provides a permeability index curve. In this case the permeability index was produced from Gamma Inversion (GI) processing, where a good match is observed between WFT pressure test mobility measurements and the NMR permeability index log (Figure 12).

Flow Units Identification (Figures 13, 14, 15, and 16)

Using the NMR permeability index and total porosity, a Modified Lorenz Plot (MLP) helped identify three key potential zones that contain nearly 60% of the total KH over the analyzed interval (Figure 13). These are labeled as Zones 3, 6, and 2 on the MLP; Zone 6 corresponds to

Layer-A, confirming it as a significant interval for production (Zones 3 and 2 on the MLP are other key producing layers in the layer-cake carbonate formations of the field but were not included in the VIT measurements). Furthermore, poro-perm plots of the data in these three zones (3, 6, and 2) indicate a common range of isopore throat sizes with a porosity range of 25 to35% and a permeability range of 3 to 30mD (Figure 14).

Improved VIT-3 Analysis Methodology

A multilayer model was created using input from the analyzed log data and the offset core data. The software used for analysis cannot analyze data from both the straddle packer and the observation probe using a multilayer model; so only the pressure data from the straddle packer was used. This still produces useful results because the pressure response at the straddle packer is affected by the communication across the multiple layers of the model.

The heterogeneity of these formations mean that the model is only an improved representation of the formation because the layers are not highly distinct, and even within the individual layers, some heterogeneity exists. This is evident on the log data and especially in the analyzed core data for Layer-A from the offset well. The multilayer model was intended to provide higher accuracy without unnecessarily high resolution and the associated complexities. It is difficult with the data available to increase the accuracy and the resolution of the model.

From the log data, the three-layer model was assumed to have a thicker bottom layer with medium-to-low permeability (Layer-C), a thin middle layer with low permeability (Layer-B) and a medium-thick upper layer with high-to-medium permeability (Layer-A) (Figure 17). The straddle packer in Layer-C is in the upper quarter of the layer, meaning that the PTA of the pressure build-up after production will perceive the impact of any permeability change in Layer-B above before it responds to a lower boundary condition. Also, based on the offset well core analysis and log data, Layer-C is reasonably homogeneous.

The pressure response through Layer-B depends on a combination of the permeability (Kxy and Kz) and the thickness. The thickness is not well defined on the log data, but it is ‘thin’ when compared to Layers A and C, meaning less than 10%, and therefore, an approximate thickness of 1 ft was used. Apart from the log data indicating the low permeability of the layer, there is one analyzed core plug from the offset well to provide an indication for the expected magnitude of the permeability.

Of the three layers, Layer-A has the most data available to define the model parameters. In addition to the log data, there is the offset well core data and the data from VIT-2, which was conducted entirely within Layer-A. However, Layer-A is also the most heterogeneous layer. The permeability distribution of the offset well core data shows high flow streaks and low flow streaks within the layer. There is also generally lower permeability at the top and bottom and higher permeability in the middle of the layer. Because the observation probe in VIT-3 is placed near the bottom of the layer, this must be accounted for in the analysis. The observation probe is affected more by the lower permeability zone at the base of the layer and does not perceive much response on the pressure build-up from the higher permeability above. The calculated permeability of VIT-2, using a homogeneous model, was Kxy=72mD and Kz=36mD (Kv/Kh ratio of 0.5). The permeability includes the high permeability over the middle zone; these values are also in agreement (similar magnitude) with the average core permeability values from the offset well. Therefore, the permeability at the observation probe is lower than this to obtain a match on the log-log derivative plot using PTA.

A simple systematic approach was used to assess the permeability of each layer by using the core data permeability average and varying it by +/-1 standard deviation. This provided an upper and lower limit for the permeability of Layers A and C. The permeability of Layer-A at the location of the observation probe was below the average permeability of the entire layer (Table 5). Other parameters for the multilayer model are displayed in Table 6.

Starting with the assumption that Layer-A has the average permeability and Layer-C has the minimum values, the data was analyzed to vary the permeability of Layer-B in order to find if a match was obtainable. In this case, no match was found, indicating that this combination is not correct (Figure 18). The result also indicates that the permeability of Layer-C is higher than the average suggested by the core analysis, if the model is to fit the data.

Increasing the permeability of Layer-C to the average value and varying the values of Layer-B also does not produce a good match, but it is clear that the late time build-up is influenced by the permeability value of Layer-B. Also, the updated plots show that the permeability of Layer-C is less than the average of the core data (Figure 19).

Decreasing the permeability of Layer-C to match the mid-time of the build-up (after the early time that is affected by tool storage and skin effects) and adjusting the permeability values of Layer-B to match the late time produces a good match with the data (Figure 20 and Table 7).

Conclusion

A quantitative analysis of the communication across the stylolite layer that connects the lower layer with the oil-water contact to the upper producing layers is important for field development. Using VITs is a cost-effective way to measure this, but because of the complexities in determining the multilayer model parameters, it is helpful to integrate other sources of data into the analysis. A few points can be made about the current dataset and the analysis.

First, the usefulness of VIT-3, across the stylolite, is demonstrated, using the data from the straddle packer in the multilayer model analysis. VIT analysis, using a homogeneous model, provides an average value, but it not ideal for thin stylolites.

Second, in VIT-3, the straddle packer gauge pressure response to the horizontal permeability (Kxy) in Layer-B and the vertical and horizontal permeability (Kz and Kxy) of Layer-A was limited. The Kz value of Layer-B was more important to the communication between Layer-A and Layer-C, and the final Kxy value for Layer-B was based on a Kv/Kh ratio of 1. The permeability values of Layer-A were adjusted to Kxy=30md and Kz=20md and were founded on the NMR data because a lower value from the core analysis was not available. The round permeability numbers were used because of the insensitivity of the pressure response to this part of the model; however, the data from VIT-2 provides a good measurement across a large section of Layer-A.

Third, accurate VIT pressure transient analysis, as indicated by the process described in this article, usually requires multiple tests to evaluate a heterogeneous formation. Careful consideration when planning VITs can greatly improve the operational efficiency, which is always a critical

factor during these tests. The location, sequence, and tool configuration are important factors to consider as well as other objectives for the WFT program, such as standard pressure tests and fluid sample collection requirements. Pre-job modeling using sensitivity analysis over ranges of expected formation and fluid parameters helps with this process.

Overall, the analysis of the VIT data included a unique approach that provided an improved quantification of the permeability across the stylolite Layer-B. In general, the use of VITs can provide useful information in a cost-effective manner, especially when a wireline formation tester is already deployed for evaluating pore pressure and obtaining fluid samples. Acquisition of the data must be carefully planned, and other data can be integrated into the analysis for a more complete analysis.

Acknowledgments

The authors thank ADMA-OPCO and Baker Hughes Incorporated for their support to complete this article.

Nomenclature

Phi	=	*porosity, fraction*
Phiz	=	*normalized porosity index, fraction*
K	=	*permeability, mD*
Kxy	=	*horizontal permeability, mD*
Kz	=	*vertical permeability, mD*
KH	=	*flow capacity, mD.ft*
FU	=	*hydraulic flow units*
RQI	=	*reservoir quality index*
FZI	=	*flow zone indicator*

Selected References

Al-Amrie, O.Y., M.A. Ben-Saad, K.I. Al Marzouqi, A.H. Kshirsagar, and S.B. Coskun, 2012, The use of formation tester to characterize the permeability and vertical communication across the stylolite zones in carbonate reservoir, *in* Sustainable Energy Growth: People, Responsibility, and Innovation.: SPE 160956-MS, Society of Petroleum Engineers, Abu Dabi International Petroleum Exhibition and Conference 2012 (ADIPEC2012), p. 666-681.

Amaefule, J. O., M. Altunbay, D. Tiab, D. D., and D. Keelan, 1993, Enhanced reservoir description using core and log data to identify hydraulic (flow) units and predict permeability in uncored intervals/wells: SPE 26436, October, SPE Annual Technical Conference and Exhibition,Houston, Texas

Earlougher, R.C., Jr., 1977, Advances in Well Test Analysis: Monograph of the Henry L. Doherty series, Society of Petroleum Engineers of AIME, Dallas.

Elarouci, F., N. Mokrani, S.M. El Djoudi, and P. Hill, 2010, How to integrate wireline formation tester, logs, core and well test data to get hydraulic flow unit permeability's: application to Algeria gas field: SPE 134001, June, SPE Production and Operations Conference and Exhibition, Tunis, Tunisia.

Gunter, G.W., J.M. Finneran, D.J. Hartmann, and J.D. Miller, 2004, Early determination of reservoir flow units using an integrated petrophysical method: SPE-38679-MS, SPE Annual Technical Conference and Exhibition, 5-8 October, San Antonio Texas.

Horne, R.N., 1995, Modern Well Test Analysis: AComputer-aided Approach: Petroway, Inc., Palo Alto, CA, 257p.

Kasap, E., and J. Lee, 1999, Analysis of wireline formation test data from gas and non-Darcy flow conditions: SPEREE, April, v.2/2, p. 116.

Kasap, E., D. G.J. Michaels, and T. Shwe, 1996, A new simplified, unified analysis of wireline formation tests sata: 37th Annual SPWLA Logging Symposium, June 16-19, p. 1-13.

Kasap, E., K. Huang, T. Shwe, and D. Georgi, 1999, Formation-rate-analysis technique: combined drawdown and buildup analysis for wireline formation test data: SPEREE, June, v.2/3, p. 273.

Lee, J., and J. Michaels, 2000, Enhanced wireline formations tests in low-permeability formations: Quality control through formation rate analysis: SPE 60293, 2000 SPE Rocky Mountain Regional/Low Permeability Reservoirs Symposium, Denver, CO, March.

Smith, C.R., G.W. Tracy, and R.L. Farrar, 1992, Applied Reservoir Engineering, v. 1 and 2: OGCI Publication, Tulsa, OK.

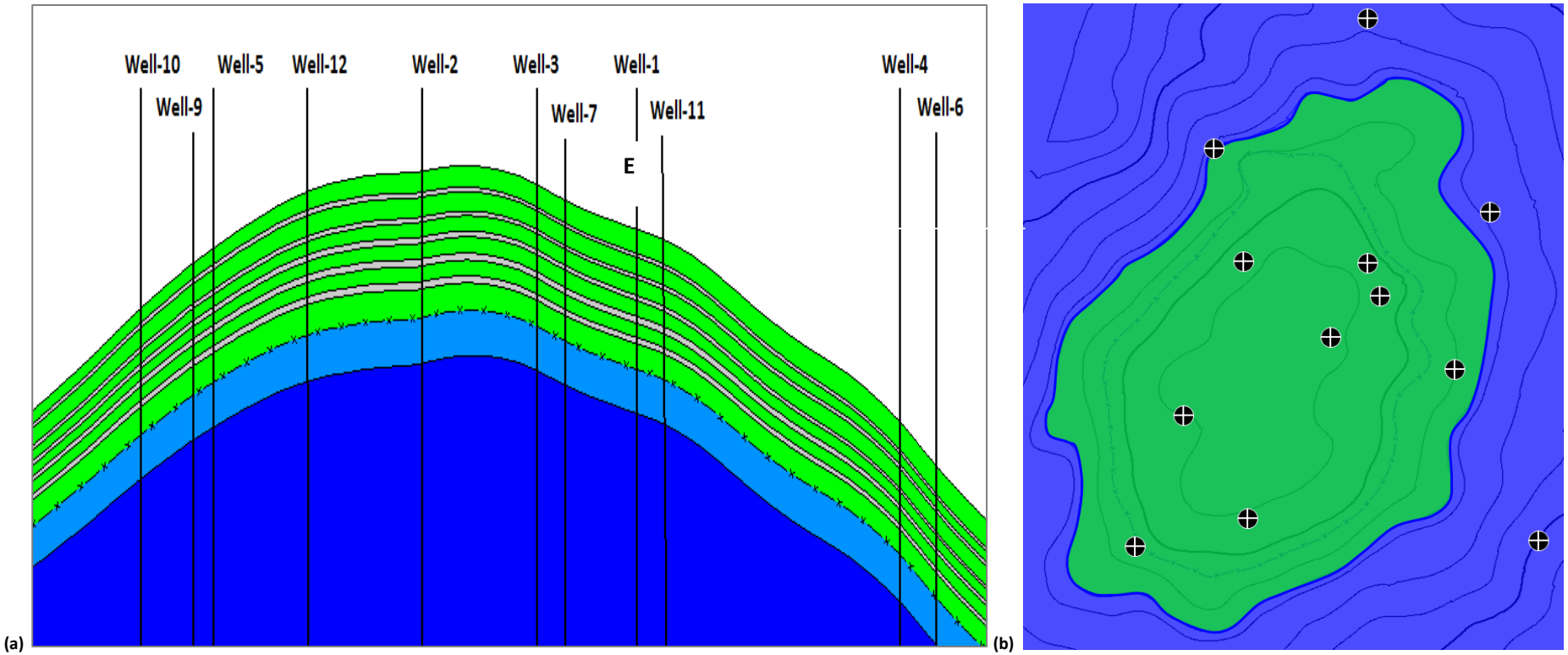

Figure 1. (a) Oil-bearing reservoir layers are pictured in light green. Grey layers are low-porosity layers within the oil zone. Light blue layer is the microporous, low-permeability layer separating the water zone from the oil zone. The dark blue layer is the permeable water zone. (b) Map of exploration and appraisal well locations and oil/water contact at top of reservoir.

Figure 2. Core image showing Layers A, B, and C.

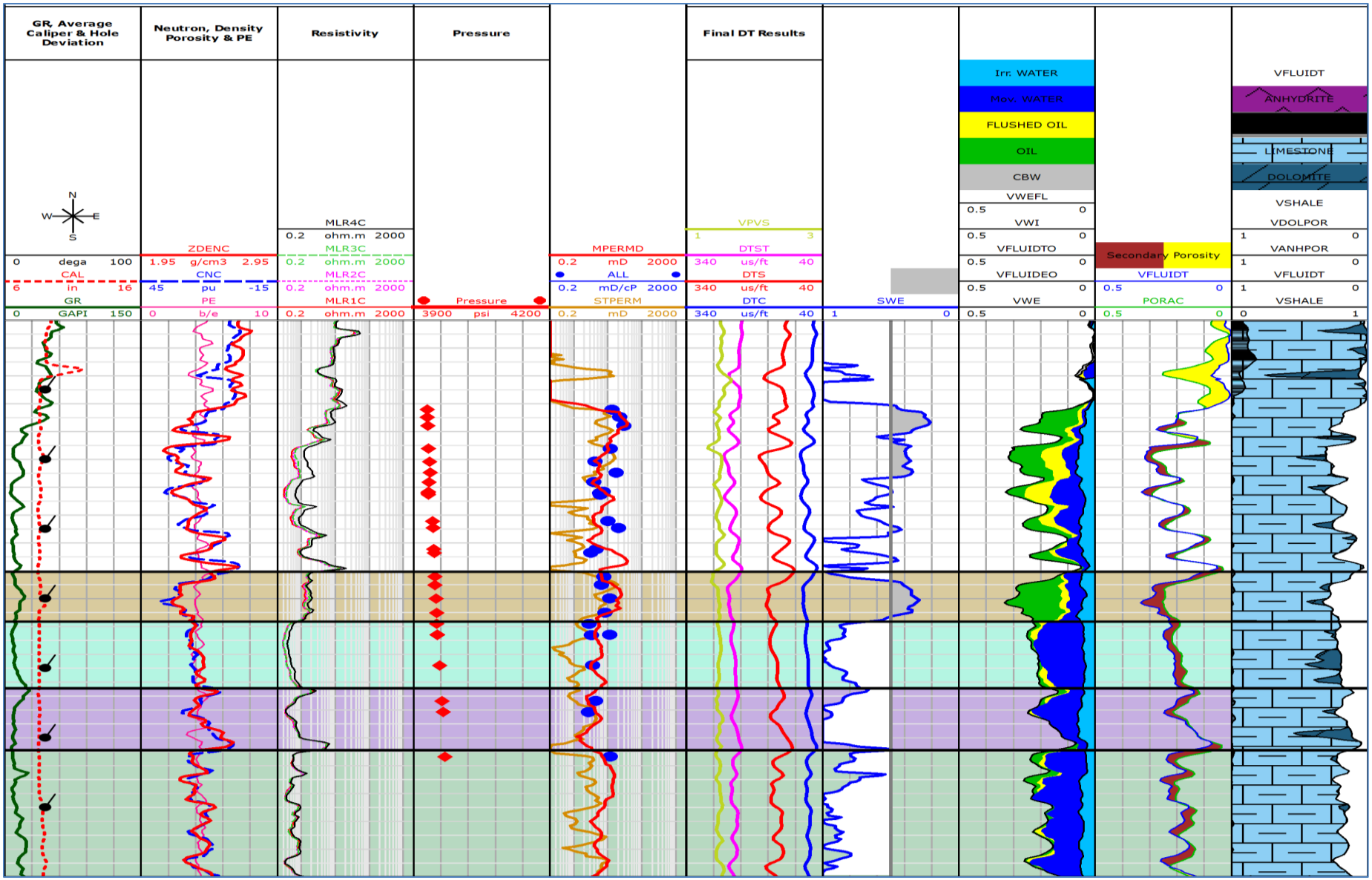

Figure 3. Plot of log data over analyzed interval with Layer-A and Layer-C identified (the thin stylolite Layer-B lies between).

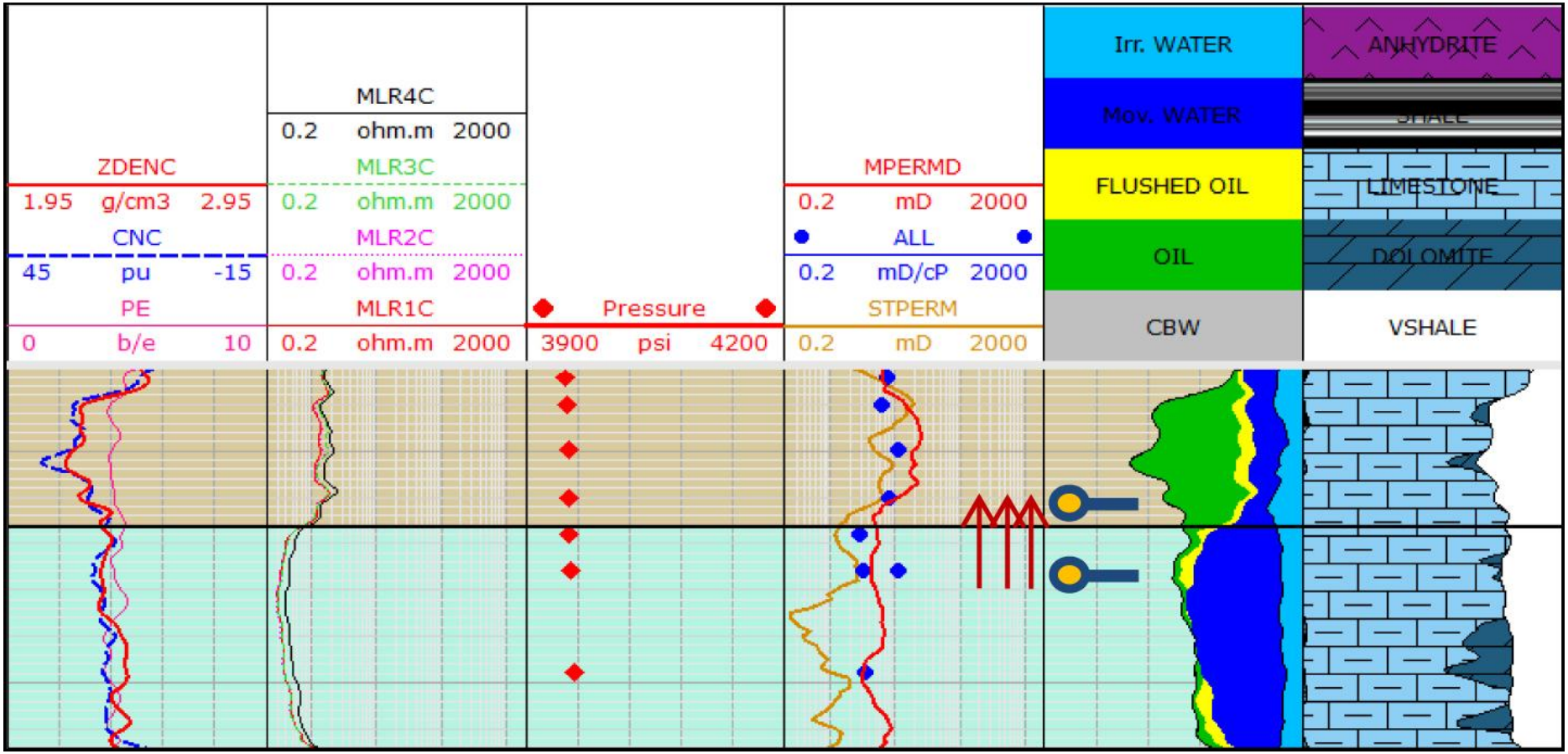

Figure 4. Probe-to-probe VIT-1 interval with producing probe in Layer-A and observation probe in Layer-C.

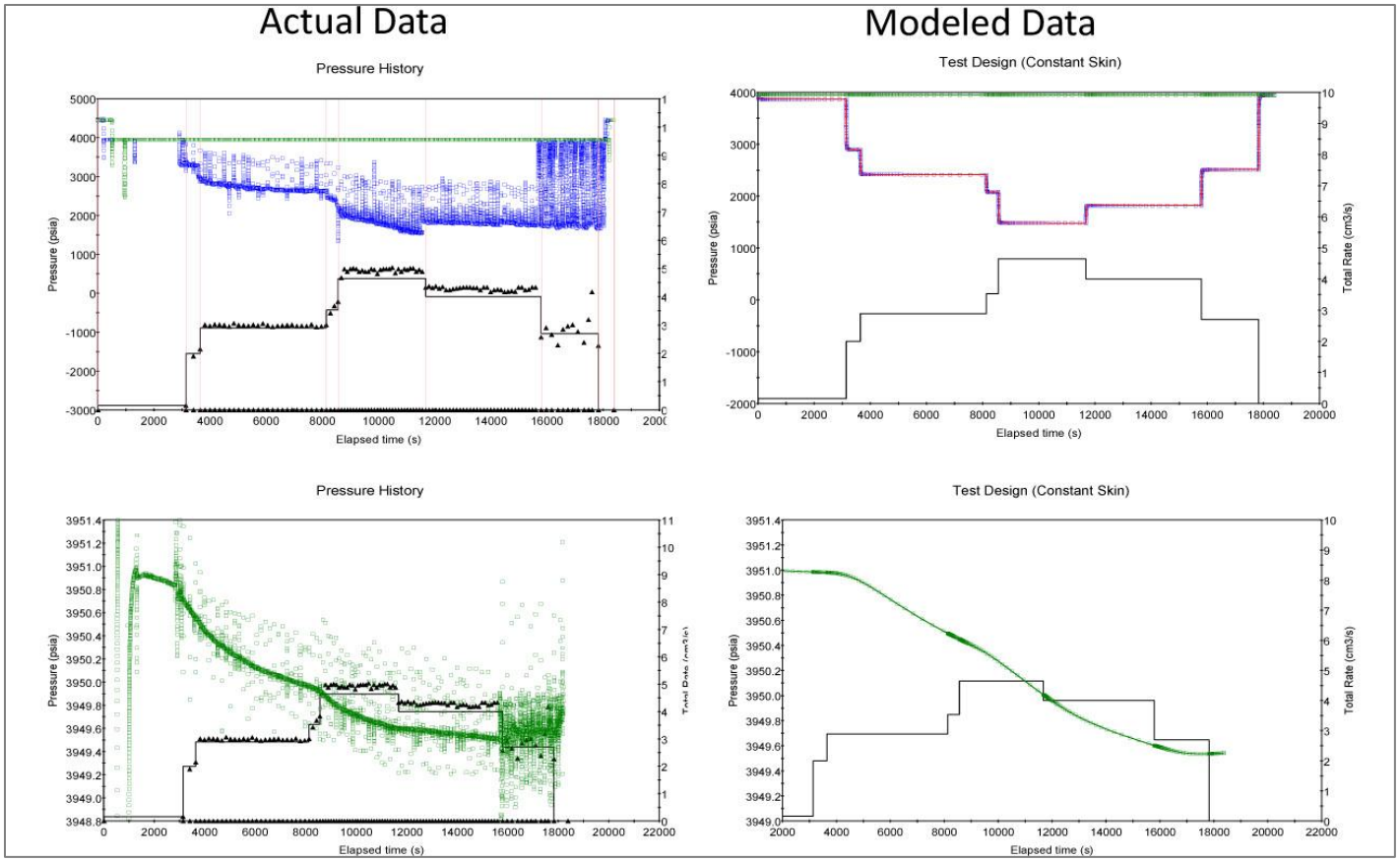

Figure 5. Actual and modeled data for VIT-1; *top-left* shows actual flowing pressure during pump-out at the producing probe (blue points) and the measured rates (black points); *bottom-left* shows actual drawdown pressure at observation probe; *top-right* shows the modeled flowing rate (black) with corresponding pressure response (red line); *bottom-right* shows the modeled pressure response at the observation probe.

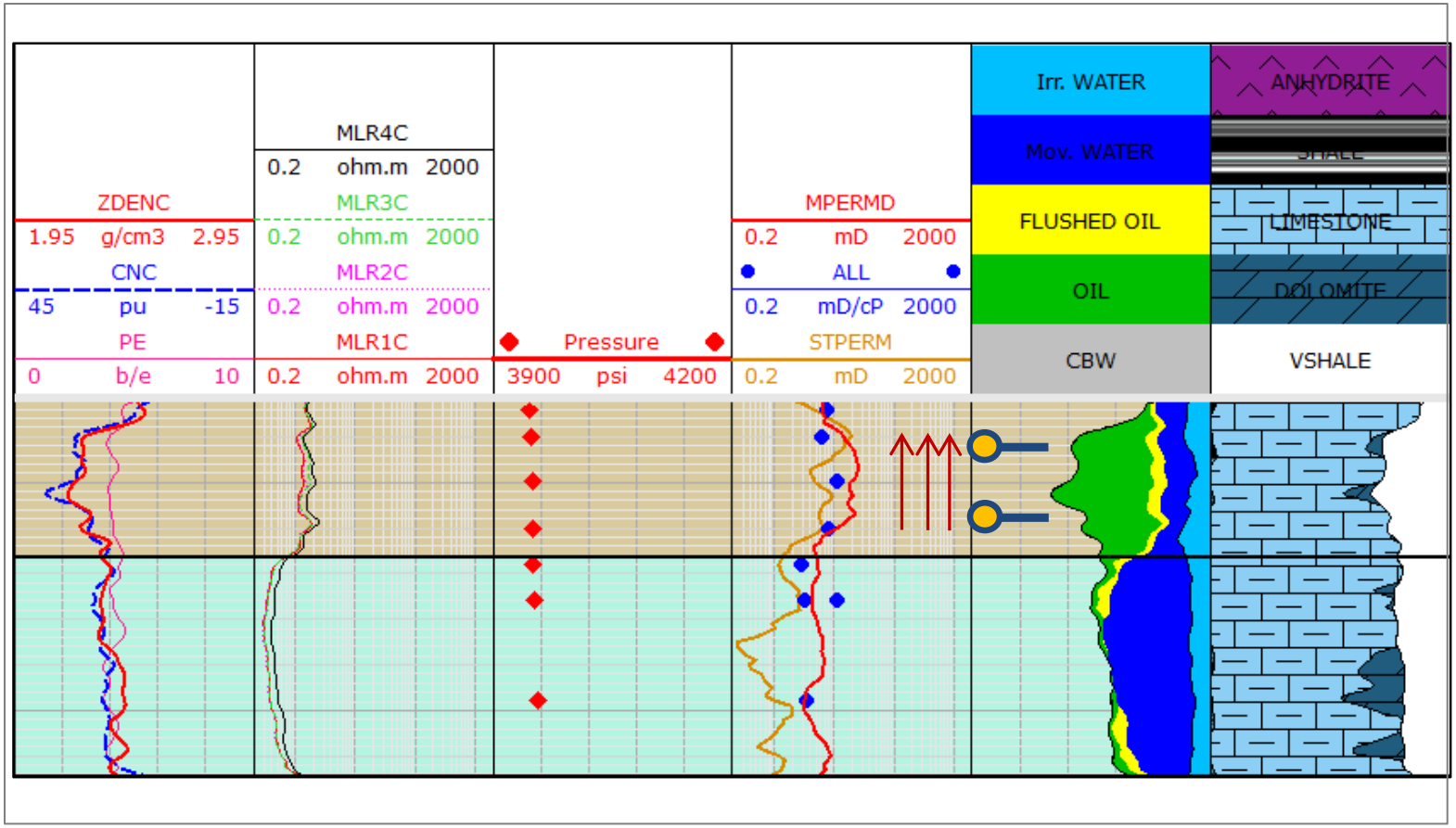

Figure 6. Probe-to-probe VIT-2 interval in Layer-A; upper probe is producing probe and lower probe is observation probe.

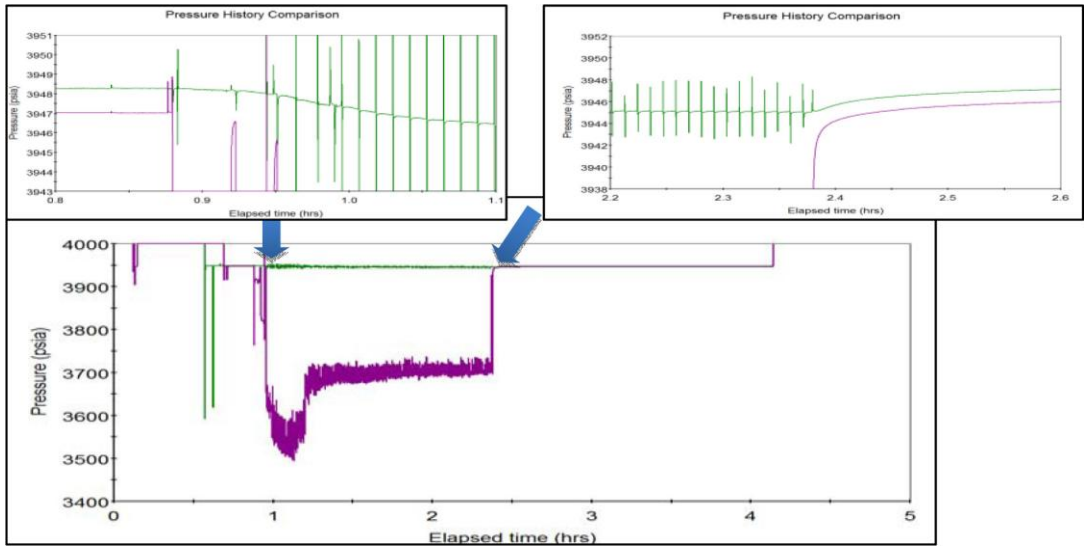

Figure 7. VIT-2 pressure at producing probe indicated in purple and observation probe pressure in green (magnified screen captures are inserted to show the pressure change on the observation probe).

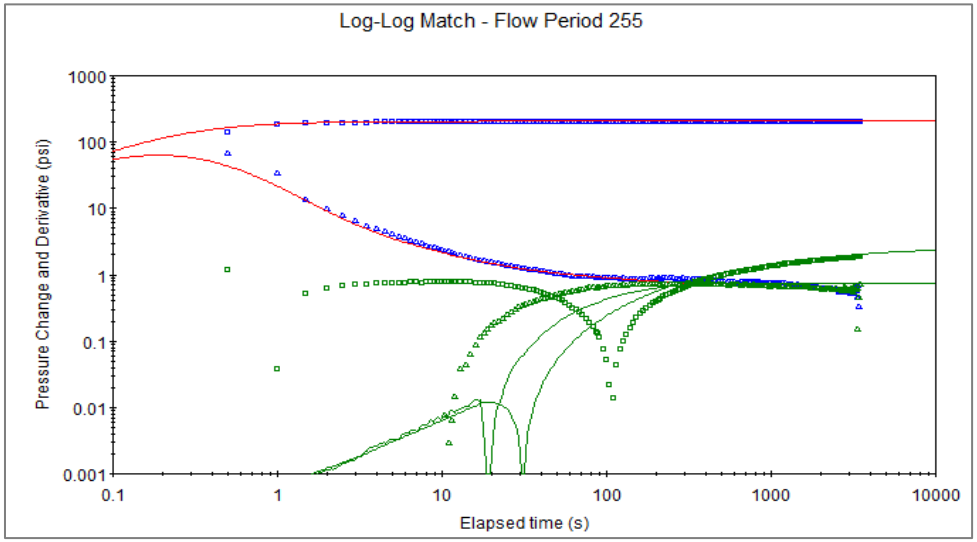

Figure 8. Log-log plot of pressure data for VIT-2; blue points indicate data from the producing probe and green points indicate observation probe data; red and green lines indicate the matched data from the homogeneous model.

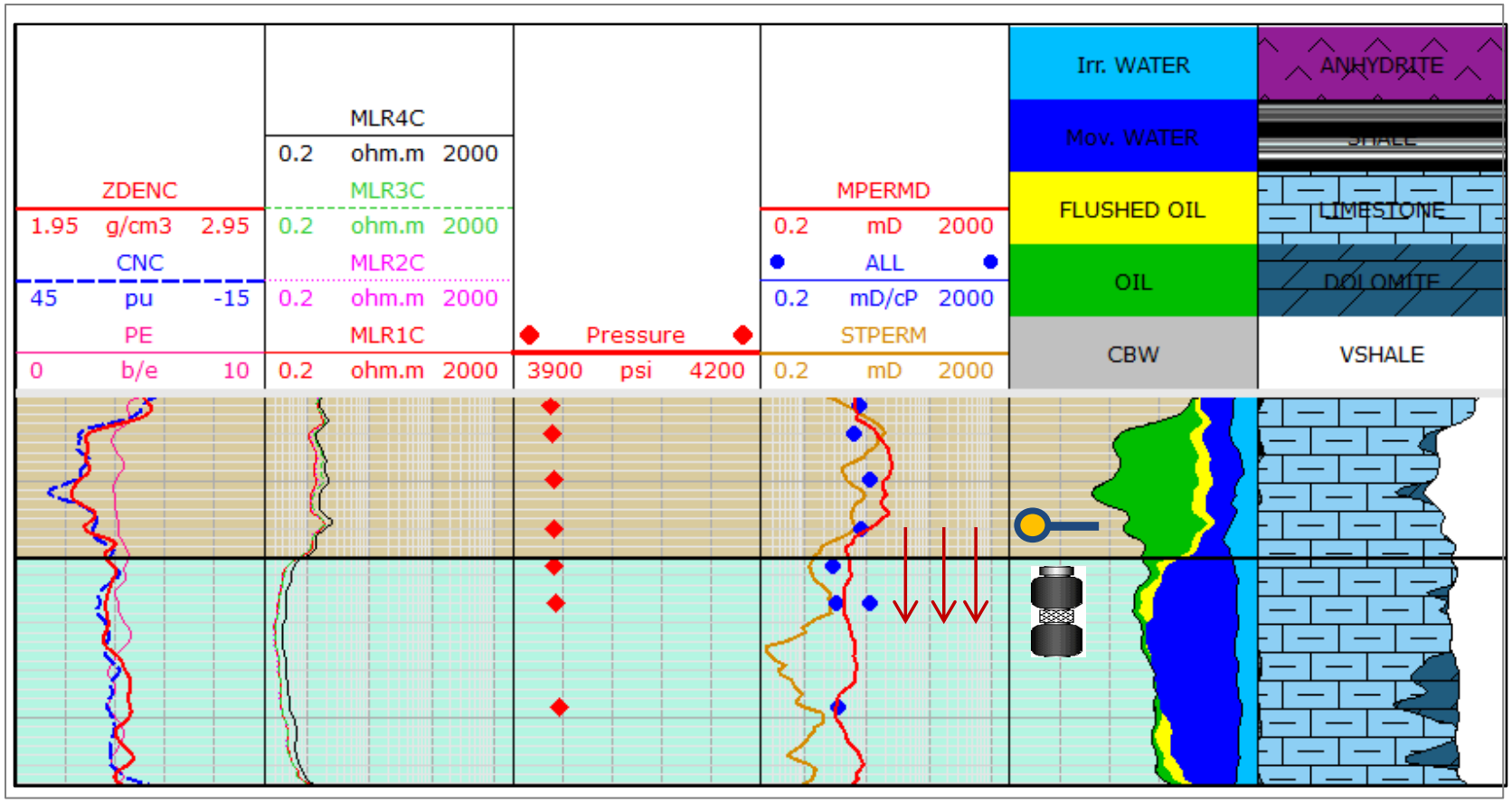

Figure 9. Log data over interval indicating Layers A, B and C and the location of the probe and straddle packer VIT-3.

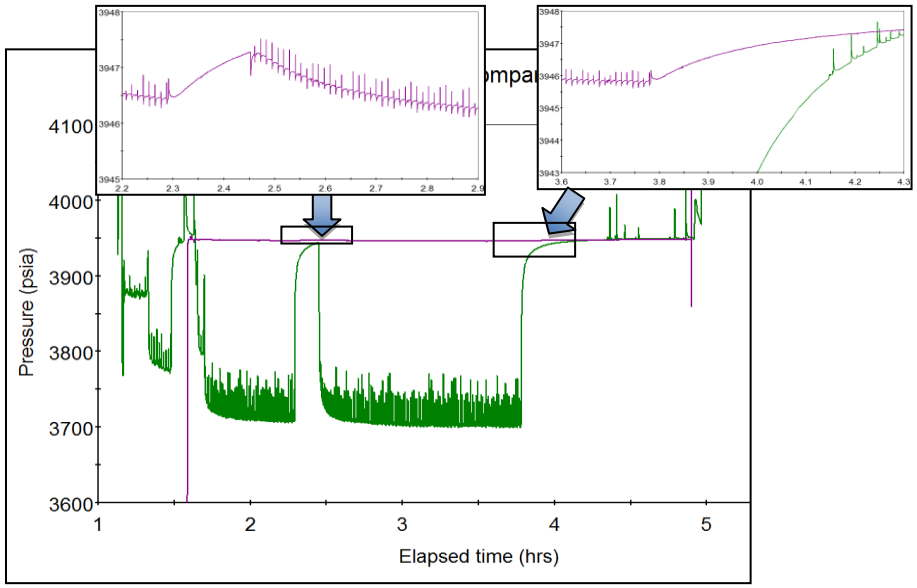

Figure 10. VIT-3 pressure at producing probe indicated in green and observation probe pressure in purple (magnified screen captures are inserted to show the pressure change on the observation probe).

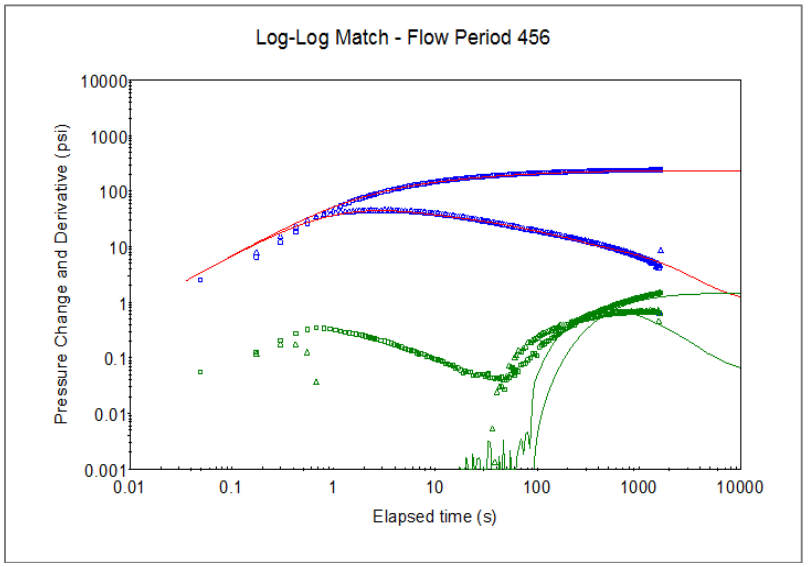

Figure 11. Log-log plot of pressure data for VIT-3; blue points indicate data from the straddle packer and green points indicate observation-probe data; red and green lines indicate the matched data from the homogeneous model.

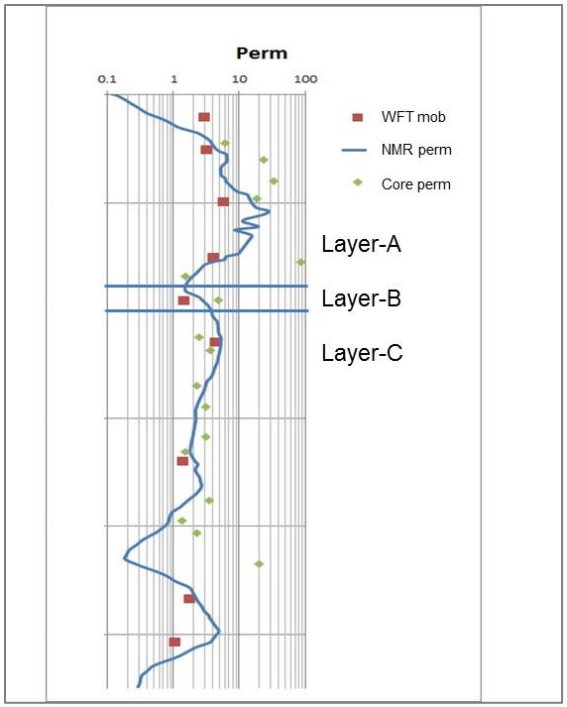

Figure 12. Composite plot of WFT mobility (red points), core permeability (green points) and NMR permeability index (blue line).

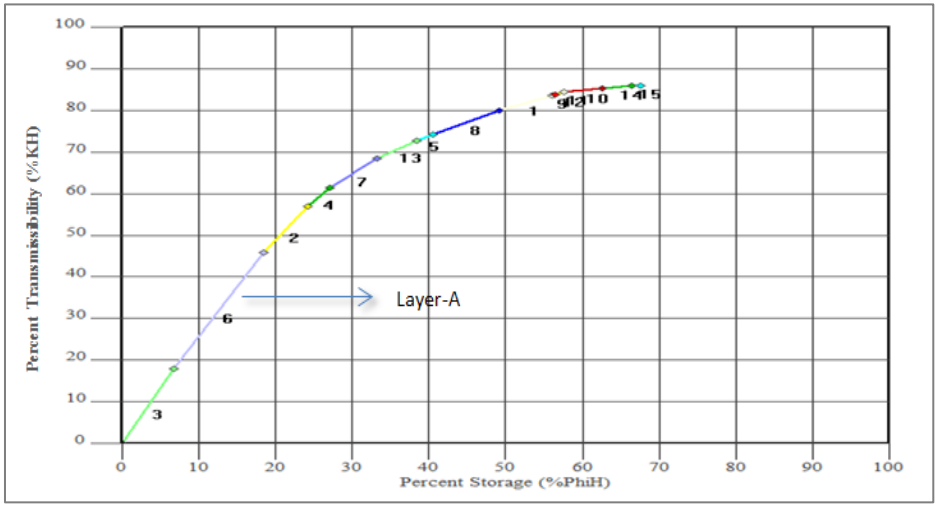

Figure 13. Modified Lorenz plot using NMR permeability and porosity.

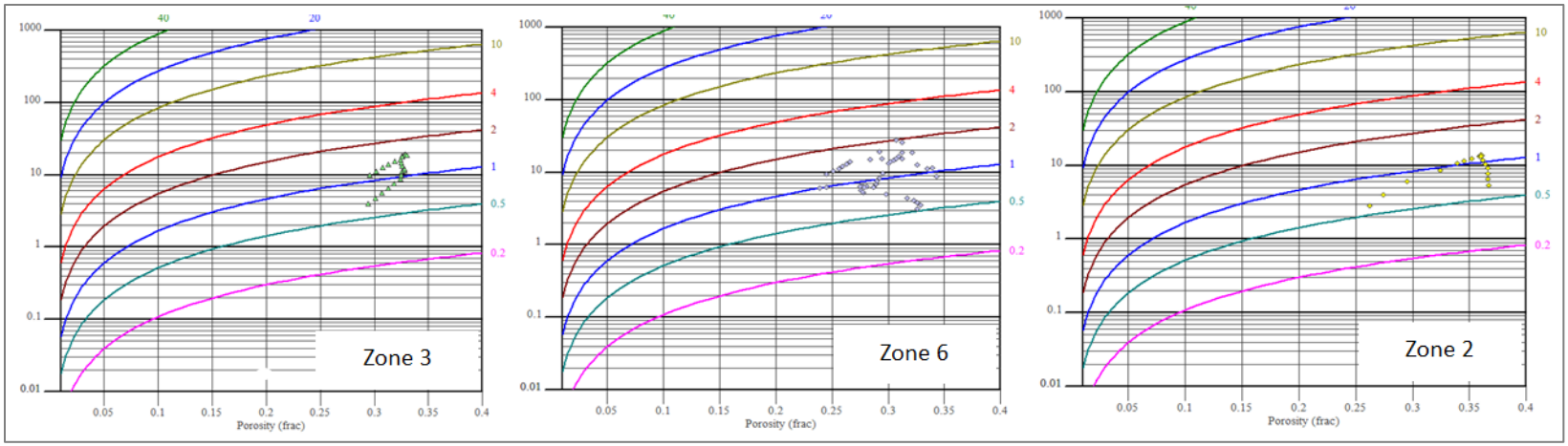

Figure 14. Poro-perm plots (normalized porosity on horizontal axis and permeability on vertical axis) for three key producing zones in the layer-cake carbonate formations with similar porosity and permeability values.

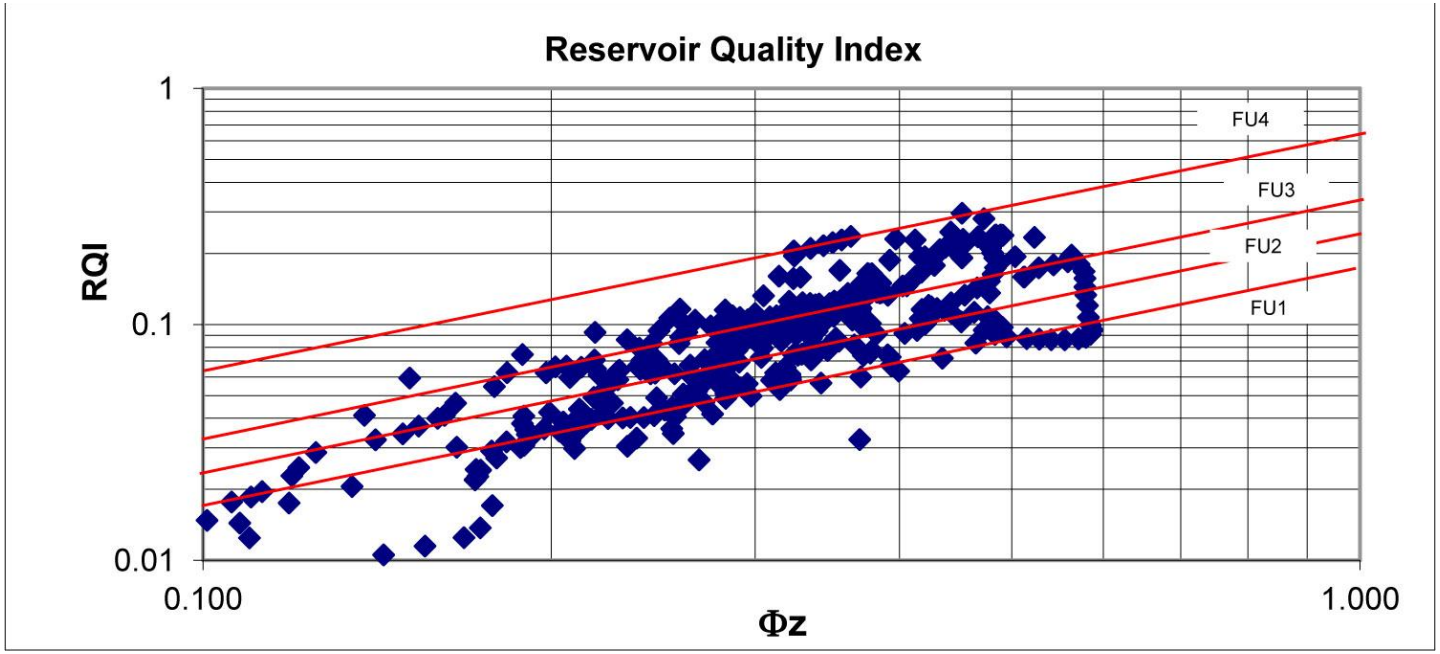

Figure 15. Reservoir Quality Index plot of NMR data over complete interval.

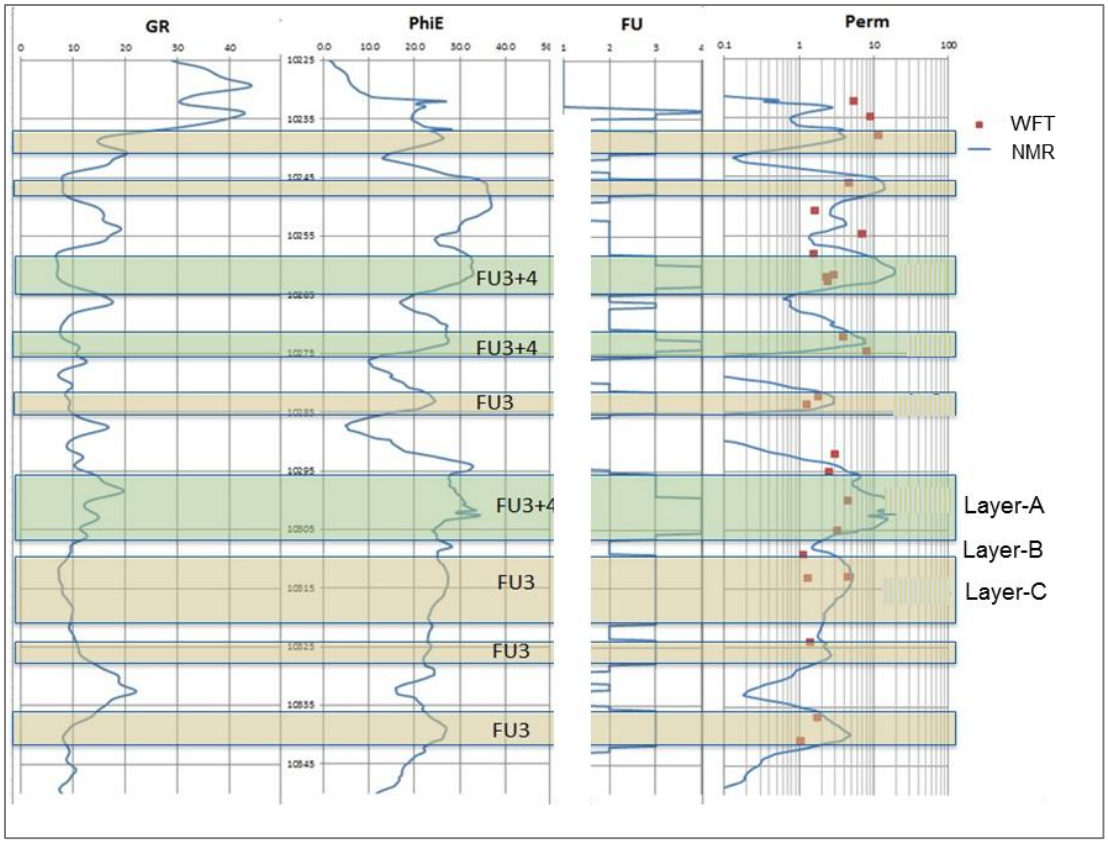

Figure 16. Plot of porosity and permeability over entire interval indicating flow units (FU) 3, 4 and 3+4; Layers A, B, and C are also identified.

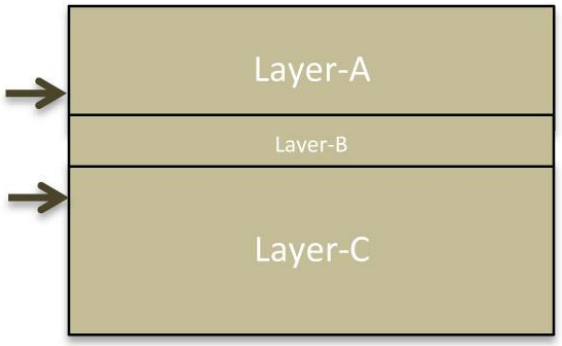

Figure 17. Multilayer model for improved analysis of VIT-3.

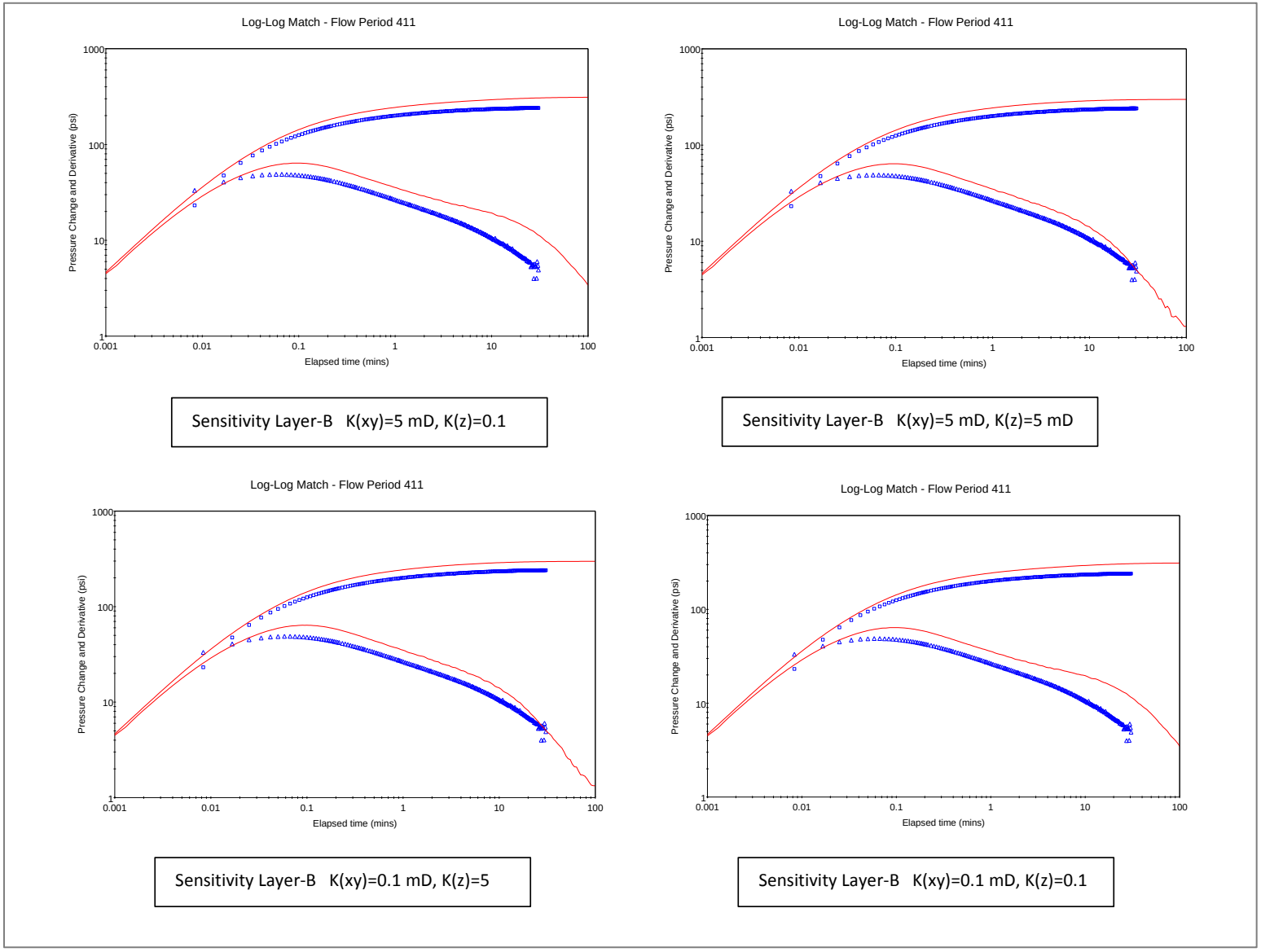

Figure 18. Log-log plot of PTA for VIT-3 using multilayer model with average permeability in Layer-A and minimum permeability in Layer-C; blue points show straddle-packer pressure data and the red lines show the match using model parameters; varying Layer-B Kxy and Kz to all combinations of expected minimum and maximum values does not produce a good match, and the data indicates that the permeability near the producing zone of the straddle packer in Layer-C is higher than the minimum suggested by the core analysis.

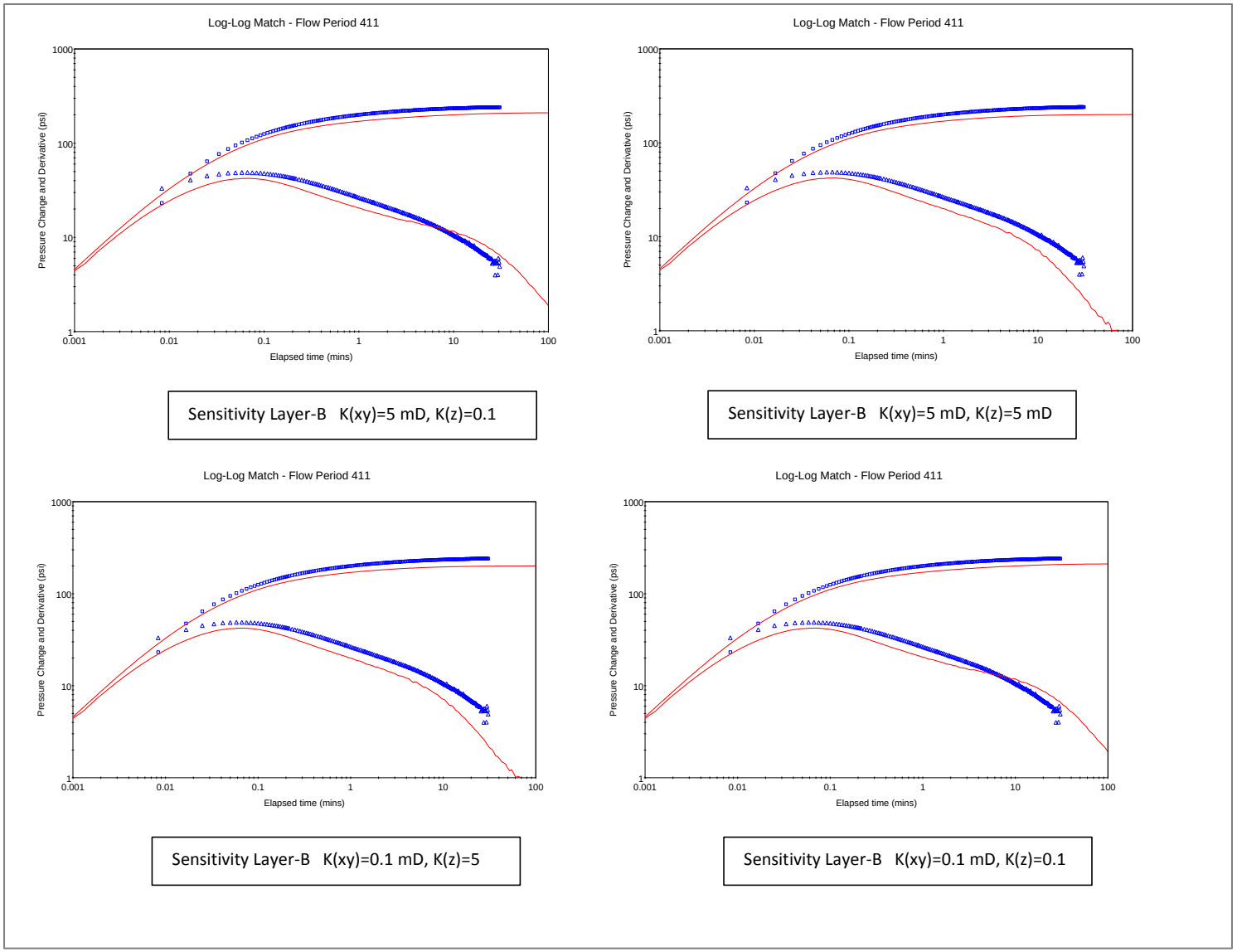

Figure 19. Log-log plot of PTA for VIT-3 using multilayer model with average permeability in Layer-A and in Layer-C; Blue points show straddle-packer pressure data, and the red lines show the match using model parameters; varying Layer-B Kxy and Kz to all combinations of expected minimum and maximum values does not produce a good match, and the data indicates that the permeability near the producing zone of the straddle packer in Layer-C is somewhat lower than the average suggested by the core analysis.

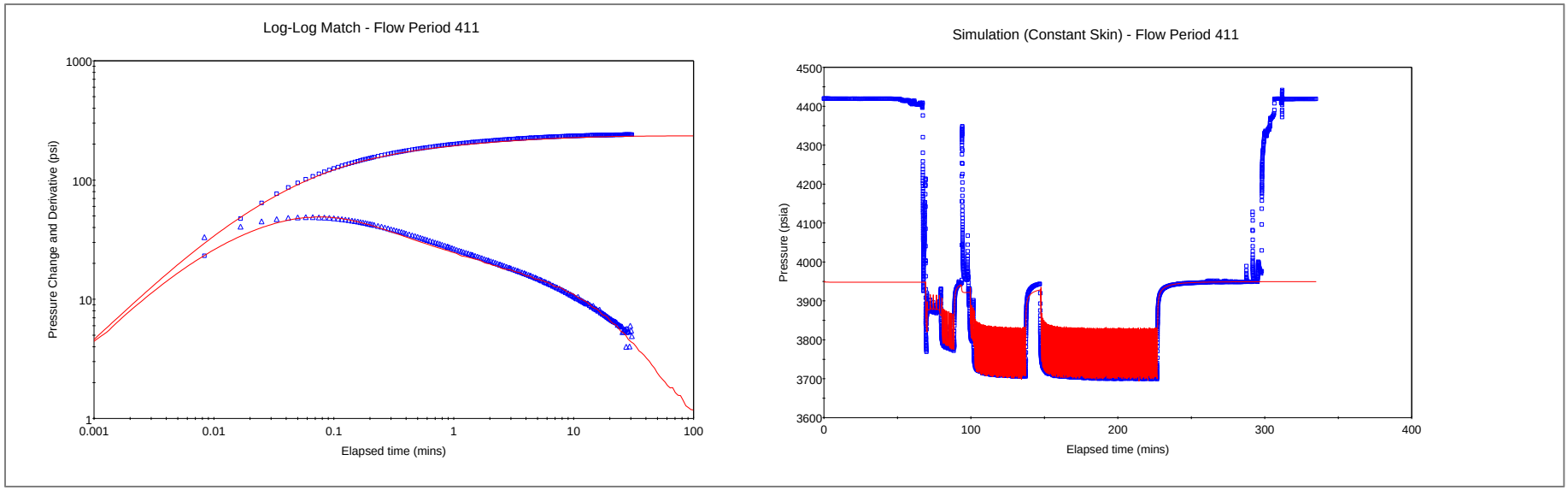

Figure 20. Log-log plot (left) and history plot (right) for VIT-3 after adjusting the permeability of Layer-C to match the mid-time and the permeability of Layer-B to match the late time; blue points indicate measured data and red lines indicate match from model.

Initial average reservoir pressure(pav)i	3950	psia
Flowing pressure, pwf	2426.5	psia
Spherical permeability k(xyz)	3.4	mD
Horizontal permeability k(xy)	4.7	mD
Vertical permeability k(z)	1.8	mD
Permeability Ratio k(z)/k(xy)	0.38	

Table 1. Summary of VIT 1 results using homogeneous model.

Initial average reservoir pressure(pav)i	3,947	psia
Flowing pressure, pwf	3,742	psia
Spherical permeability k(xyz)	57	mD
Horizontal permeability k(xy)	72	mD
Vertical permeability k(z)	36	mD
Permeability ratio k(z)/k(xy)	0.5	
Distance to top boundary dTop (producing probe)	5	ft
Distance to bottom boundary dBottom (producing probe)	10	ft
Type top	No Flow	
Type bottom	No Flow	

Table 2. Summary of VIT-2 analysis using homogeneous model

Initial average reservoir pressure, (pav)i	3948	psia
Horizontal Permeability, k(xy)	3.939	mD
Vertical permeability, k(z)	1.801	mD
Type of top boundary	No Flow	
Type of bottom boundary	No Flow	

Table 3. Summary of VIT-3 analysis using homogeneous model.

	Depth	Porosity	Kair (Kxy)	Depth	Kair (Kv)
Layer-A	x04.50	20.4	6.1	x05.55	17.
	x06.00	30.4	23.	x07.85	89.
	x08.00	27.4	33.	x09.85	12.
	x09.60	21.4	18.	x13.85	31.
	x14.10	29.4	142.		
	x15.50	34.8	88.		
	Ave	**27.29**	**51.95**		**37.40**
	Std Dev	**5.55**	**52.65**		**35.02**
Layer-B	x16.80	20.2	1.5	x17.00	1.7
Layer-C	x19.00	25.7	4.7	x19.20	2.8
	x22.50	23.0	2.4	x22.70	3.3
	x23.70	23.9	3.7	x23.95	2.2
	x27.00	20.5	2.2	x27.25	3.0
	x28.90	20.7	3.1	x28.70	3.2
	x31.70	19.5	3.1	x31.95	2.1
	x33.10	18.4	1.5	x33.33	1.6
	x37.60	19.7	3.4	x37.80	1.8
	x39.50	17.7	1.3	x39.65	3.4
	x40.60	22.6	2.3	x40.75	3.2
	Ave	**21.17**	**2.79**		**2.68**
	Std Dev	**2.57**	**1.03**		**0.67**

Table 4. Depth-matched core data from offset well over layers A, B, and C.

Layer-A	Min	Ave	Max
Kxy	NA	51.95	104.60
Kz	NA	37.40	72.42
Layer-C	Min	Ave	Max
Kxy	1.76	2.79	3.82
Kz	2.01	2.68	3.35

Table 5. Initial range of permeability values for Layers A and C, based on core analysis and standard deviations.

Distance from reservoir bottom to straddle packer, Zw	16.8	ft
Distance between straddle packer and observation probe	9.5	ft
Completed interval	3	ft
Layer-A thickness	15	ft
Layer-B thickness	1	ft
Layer-C thickness	19	ft
Layers A, B and C Porosity	0.28, 0.2, 0.18	fraction
Layers A, B and C fluid viscosity	1.5, 1.5, 1.5	cP
Layers A, B and C compressibility	3.7E-5, 3.7E-5, 1.4E-6	1/psi
Average reservoir pressure	3950	psia
Average reservoir temperature	200	deg.F
Water formation volume factor, Bw	1	RB/STB
Water Viscosity, Muw	0.5	cP
Oil Compressibility, Co	1.42E-05	1/psi
Gas Compressibility, Cg	0.00016575	1/psi
Water Compressibility, Cw	3.31E-06	1/psi
Formation Compressibility, Cf	3.10E-06	1/psi
Oil Saturation, So	7.00E-01	fraction
Water Saturation, Sw	3.00E-01	fraction
Total Compressibility, Ct	2.14E-05	1/psi

Table 6. Summary of input parameters for multilayer model.

Initial average reservoir pressure, (pav)i	3950	psia
Flowing pressure, pwf	3708	psia
Total permeability thickness, kh	496.3	mD.ft
Average permeability, k(av)	14.18	mD
Perforated interval , Hw	3	ft
Wellbore skin factor, S(w)	-1.20	
Distance to lower boundary, Zw	14	
Wellbore storage coefficient, C	1E-006	Bbl/psi
Layer A horizontal permeability, k1 (xy),	30	mD
Layer B horizontal permeability, k2 (xy),	0.4	mD
Layer C horizontal permeability, k3 (xy)	2.4	mD
Layer A vertical permeability, k1 (z),	20	mD
Layer B vertical permeability, k2 (z)	0.4	mD
Layer C vertical permeability, k3 (z),	2.3	mD
Radius of investigation (approx), ri	38	ft
Measured productivity index, PI	0.03211	B/D/psi

Table 7. Final results for VIT-3 using multilayer model.